

Search for $2p$ decay of the first excited state of ^{17}Ne

P. G. Sharov,^{1,2,*} A. S. Fomichev,^{1,3} A. A. Bezbakh,^{1,2} V. Chudoba,^{1,4} I. A. Egorova,^{5,2} M. S. Golovkov,^{1,3} T. A. Golubkova,^{6,2} A. V. Gorshkov,^{1,2} L. V. Grigorenko,^{1,7,8} G. Kaminski,^{1,9} A. G. Knyazev,^{1,2} S. A. Krupko,^{1,2} M. Mentel,^{1,10} E. Yu. Nikolskii,^{7,1} Yu. L. Parfenova,^{1,11} P. Pluchinski,^{1,10} S. A. Rymzhanova,^{1,2} S. I. Sidorchuk,¹ R. S. Slepnev,¹ S. V. Stepantsov,¹ G. M. Ter-Akopian,^{1,3} and R. Wolski^{1,9}

¹Flerov Laboratory of Nuclear Reactions, JINR, Dubna, RU-141980, Russia

²SSC RF ITEP of NRC “Kurchatov Institute”, Moscow RU-117218, Russia

³Dubna State University, Dubna RU-141982, Russia

⁴Institute of Physics, Silesian University in Opava, 74601 Opava, Czech Republic

⁵Bogoliubov Laboratory of Theoretical Physics, JINR, Dubna, RU-141980, Russia

⁶Advanced Educational and Scientific Center, Moscow State University, Kremenchugskaya 11, 121357 Moscow, Russia

⁷National Research Center “Kurchatov Institute”, Kurchatov sq. 1, RU-123182 Moscow, Russia

⁸National Research Nuclear University “MEPhI”, Kashirskoye shosse 31, 115409 Moscow, Russia

⁹Institute of Nuclear Physics PAN, Radzikowskiego 152, PL-31342 Kraków, Poland

¹⁰AGH University of Science and Technology, Faculty of Physics and Applied Computer Science, al. Mickiewicza 30, 30-059 Krakow, Poland

¹¹Skobeltsyn Institute of Nuclear Physics, Moscow State University, 119991 Moscow, Russia

(Received 13 June 2017; published 28 August 2017)

Two-proton decay of the ^{17}Ne low-lying states populated in the $^1\text{H}(^{18}\text{Ne},d)^{17}\text{Ne}$ transfer reaction is studied. The two-proton width Γ_{2p} of the ^{17}Ne first excited $3/2^-$ state at $E^* = 1.288$ MeV is of importance for the two-proton radioactivity theory and nuclear-astrophysics applications. A dedicated search for the two-proton emission of this state was performed leading to the new upper limit obtained for the width ratio $\Gamma_{2p}/\Gamma_\gamma < 1.6(3) \times 10^{-4}$. An original, “combined mass” method is suggested and tested as capable of improving the resolution of the experiment, which is a prime significance for the study of nuclear states with extremely small particle-to-gamma width ratios $\Gamma_{\text{part}}/\Gamma_\gamma$. The condition $\Gamma_{\text{part}} \ll \Gamma_\gamma$ is quite common for the states of astrophysical interest, which makes the proposed approach promising in this field.

DOI: [10.1103/PhysRevC.96.025807](https://doi.org/10.1103/PhysRevC.96.025807)

I. INTRODUCTION

One of the most important tasks for nuclear studies in astrophysics is the measurement of various reaction rates for nucleosynthesis calculations. In particular, for the important situation of the *resonant* particle radiative capture the reaction rate of the selected resonant state at temperature T is proportional to

$$\langle\sigma_{\text{part},\gamma}\rangle(T) \sim \frac{1}{T^{3n/2}} \exp\left(-\frac{E_r}{kT}\right) \frac{\Gamma_\gamma \Gamma_{\text{part}}}{\Gamma_{\text{tot}}}, \quad (1)$$

where E_r is the resonance position, Γ_γ and Γ_{part} are partial widths of the resonance E_r into gamma and particle channels [1]. The “particle” here can be proton, alpha, two protons, and so on, and n is the number of captured particles: 1 for p, α and 2 for $2p$ captures. The total width of the resonance in the majority of cases is defined as $\Gamma_{\text{tot}} = \Gamma_\gamma + \Gamma_{\text{part}}$. Therefore in all such cases there are just two values needed to define the resonance contribution to the radiative capture rate: (i) the resonance energy E_r and (ii) the ratio $\Gamma_{\text{part}}/\Gamma_{\text{tot}}$. For the resonant states situated well below the Coulomb barrier particle width can be very small; this ratio then becomes effectively equal to $\Gamma_{\text{part}}/\Gamma_\gamma$, and its determination becomes a complicated task.

Reaction studies provide a way to determine the $\Gamma_{\text{part}}/\Gamma_{\text{tot}}$ ratio without γ measurements. The comparison of data

obtained in the measurements made for the missing mass and invariant mass spectra represents one of the possible ways to obtain the $\Gamma_{\text{part}}/\Gamma_\gamma$ ratio. The missing mass spectrum allows the definition of the population cross section for the state of interest, while the invariant mass spectrum provides the decay cross section into the particle channel. The ratio of these cross sections is evidently equal to $\Gamma_{\text{part}}/(\Gamma_{\text{part}} + \Gamma_\gamma)$.

In this work we address the subject of the extremely weak $2p$ decay branch of the first excited $3/2^-$ state of ^{17}Ne , which is known [2,3] to predominantly undergo γ decay to the ground state. In Sec. II we discuss some issues of the ^{17}Ne study in general and then return to the subject of measuring the extremely small $\Gamma_{\text{part}}/\Gamma_\gamma$ ratio in Sec. III. Further in this work, we study experimentally the $^1\text{H}(^{18}\text{Ne},d)^{17}\text{Ne}$ reaction and derive a new upper limit for the $\Gamma_{2p}/\Gamma_\gamma$ ratio of the $3/2^-$ state. Instead of the *invariant mass* method to determine the $2p$ -decay rate we use the original *combined mass* method to provide better experimental resolution. In Sec. VII we demonstrate the prospects of the developed method in forthcoming experiments to reduce this limit to the range where, according to theoretical predictions, the direct observation of the $3/2^-$ state $2p$ decay becomes realistic.

II. PROBLEMS OF ^{17}Ne STUDIES

Neon-17 is a kind of “conundrum nucleus” whose structure and reactions attracted a lot of interest. Multiple efforts to

*Corresponding author: sharovpavel@jinr.ru

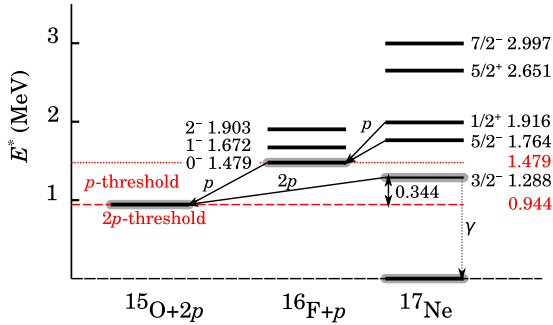


FIG. 1. The level schemes for ^{17}Ne , its one-proton subsystem ^{16}F , and decay scheme for ^{17}Ne states.

investigate it, both theoretically and experimentally, have not yet provided convincing clarity about its properties. There are several questions of special interest connected with this nucleus that are actually tightly interwoven.

The ^{17}Ne nucleus sits on the proton dripline and it is relatively loosely bound with respect to the $2p$ breakup ($E_b = 944$ keV, see Fig. 1). This is a borromean nucleus: its ^{16}F subsystem is unbound with $S_p(^{16}\text{F}) = -535$ keV. The situation with ^{17}Ne separation energies is highly analogous to that with the “classical” two-neutron halo nucleus ^6He and thus the question about the existence of the two-proton halo in ^{17}Ne was formulated in Ref. [4]. The intrigue of this problem is enhanced by the fact that the ^{17}Ne nucleus is probably the only realistic candidate to possess a two-proton halo as in heavier proton dripline systems the specific spatial extension of the valence nucleon wave functions should be suppressed by the Coulomb interaction. The issue of the two-proton halo in ^{17}Ne was discussed in the theory papers [5,6] and experimental works [7,8].

The ^{15}O nucleus is a “waiting point” in the astrophysical rp-process as its half-life $T_{1/2} = 122.24$ s is comparable to the timescale of the typical rp-process scenarios. The radiative absorption of two protons ($2p$ capture) is known to be a possible bypath for this waiting point [9]. The so far unknown $2p$ decay width of the first excited state of ^{17}Ne ($E^* = 1288$ keV, $J^\pi = 3/2^-$) makes a key point for solving the bypass problem of the ^{15}O waiting point. Taking into account this (previously omitted) state in the calculation of the *resonant* radiative capture rate strongly modified the corresponding rate in a broad temperature range around 0.15 GK [10]. This modification is as large as 3–8 orders of magnitude, where the variation corresponds to the uncertainty in $2p$ width predicted in theory works [10,11] for the 1.288 MeV $3/2^-$ state.

There is considerable interest in studies of the $2p$ decay of the $3/2^-$ state from the nuclear theory side as well. The two-proton decay energy of the first excited state in ^{17}Ne is only $E_T = -S_{2p}(^{17}\text{Ne}) = 344$ keV. This state of ^{17}Ne belongs to the class of so-called “true” two-proton emitters [12]. Here the protons should be emitted simultaneously because the narrow ($\Gamma \sim 40$ keV) ground state of the intermediate ^{16}F system at $E_r = 535$ keV is not accessible for sequential decay. Due to the very small $2p$ decay energy E_T , the two-proton decay of ^{17}Ne should have a typical radioactivity-scale lifetime. For many years preceding the discovery of the ground state $2p$

radioactivity in heavier proton dripline nuclei ^{45}Fe , ^{48}Ni , and ^{54}Zn [Ref. [12], and references therein], the first excited state of the ^{17}Ne nucleus remained among the prime candidates for the discovery of $2p$ radioactivity.

The shell-model calculation using the Warburton and Brown interaction led to an estimated partial decay width of 5.5×10^{-9} MeV for the γ decay of ^{17}Ne $3/2^-$ state [13]. The $2p$ decay from the $3/2^-$ state to the $1/2^-$ ground state of ^{15}O can proceed only via the escape of the *sd*-shell proton pair. Few-body calculations performed in the two different theoretical approaches predicted the two-proton decay width to be $\Gamma_{2p} \sim (5 - 8) \times 10^{-15}$ MeV [11] or $\Gamma_{2p} = 1.4 \times 10^{-14}$ MeV [14]. For the first excited state of ^{17}Ne this gives a ratio of $\Gamma_{2p}/\Gamma_{\text{tot}} \approx \Gamma_{2p}/\Gamma_\gamma$ to be $(0.9 - 2.5) \times 10^{-6}$.

Up to now only an upper limit of this value is known [15]. From the nonobservation of the two-proton emission from the $3/2^-$ state a one-sigma upper limit for the branching ratio $\Gamma_{2p}/\Gamma_\gamma \leq 7.7 \times 10^{-3}$ was set.

III. EXPERIMENTAL APPROACH

The searched $\Gamma_{2p}/\Gamma_\gamma$ branching ratio for the $2p$ decay of the ^{17}Ne $3/2^-$ state is expected to be located in a broad band of values from the experimental limit $\Gamma_{2p}/\Gamma_\gamma < 7.7 \times 10^{-3}$ to the theoretical predictions $\Gamma_{2p}/\Gamma_\gamma \sim 9 \times 10^{-7}$. The primary purpose of this work is to reduce the experimental limit as much as possible and to test the suggested combined mass method.

The one-neutron transfer reaction $^1\text{H}(^{18}\text{Ne},d)^{17}\text{Ne}$ is the subject of study in this work. The measurement of the missing mass spectrum provides the *population rates* for the ^{17}Ne states. Standard methodology implies that, turning to the measurement of the invariant mass spectrum, one can detect the yield of a weak $2p$ -decay branch inherent to the state of interest which is the $3/2^-$ state of ^{17}Ne . Naturally, the revelation of the tiny particle-decay branch of the lower-lying $3/2^-$ state requires special attention to the reduction of the background coming from the strong particle-decay branch of the higher-lying $5/2^-$ or/and $1/2^+$ states.

There are two ways to overcome this problem. (i) Choose the reaction that provides the highest ratio for the population of the state of interest with respect to the nearest states which can seed background events in the energy range of interest. (ii) Maximal increase of the experimental resolution, so that the background events connected with the nearest states are well separated from the energy range of interest.

Deciding in favor of the $^1\text{H}(^{18}\text{Ne},d)^{17}\text{Ne}$ reaction one can benefit from the fact that the nearest state to $3/2^-$, the $5/2^-$ state, is expected to be poorly populated in this reaction. Distorted-wave Born approximation (DWBA) calculations (see Sec. V for the parameters) show the average cross section for the $5/2^-$ state, taken in a proper range center-of-mass angle, being more than one order of magnitude less than that for the $3/2^-$ state.

To enable the better selection of the desired ^{17}Ne state we used an original approach that was named the combined mass method. The measurement of the emission angle and energy of recoil deuteron appearing in this reaction is the

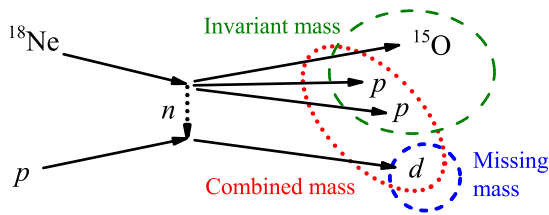


FIG. 2. The illustration of missing mass, invariant mass, and combined mass methods for the $^1\text{H}(^{18}\text{Ne},d)^{17}\text{Ne}$ reaction.

prerequisite to the realization of this approach. Figure 2 is destined to illustrate, on the example of the $^1\text{H}(^{18}\text{Ne},d)^{17}\text{Ne}$ reaction, the choice of particles to be detected in the combined mass method. Of course, this is the only objective when the excitation spectrum of ^{17}Ne is measured by the missing mass method. The yields of different resonance states are defined by this method irrespective of their decay modes. The detection of the recoil deuteron in coincidence with protons only offers a way to the yield determination made for the decay branches of the ^{17}Ne excited states associated with the proton emission. Certainly, of particular interest here is the search for the anticipated very weak two-proton decay branch of its first excited state ($E^* = 1288$ keV, $J^\pi = 3/2^-$).

In the proposed approach the ability to select rare $2p$ -decay events of the $3/2^-$ state in ^{17}Ne is improved due to the considerable mass asymmetry for the particles both in the reaction ($A_d/A_{^{17}\text{Ne}} = 2/17$) and in the decay ($A_{2p}/A_{^{15}\text{O}} = 2/15$) channels. In the $d - ^{17}\text{Ne}$ center-of-mass system the velocity of the heavier particle ($^{17}\text{Ne}^*$) is known with the precision better by a factor of $17/2$ than that for the lighter one (deuteron). The energies of the emitted protons in the ^{17}Ne center of mass are defined with much better accuracy. So, having measured in a laboratory system the emission angle of the recoil deuteron even with a modest (about one degree) precision one specifies with a tremendous accuracy (within $\Delta E/E \approx 6 \times 10^{-4}$ and better than 0.1 degree, respectively) the energy and escape direction of ^{17}Ne . It should be noted that such a situation is typical, in general, for the study of transfer reactions made in inverse kinematics with heavy projectiles bombarding light target nuclei. The resolution attainable by means of the combined mass method for the excitation energy spectrum depends on the target thickness, which can be set to be quite large due to the small specific energy loss of the protons which are due to detection. This favors the revelation of such small $2p$ decay branch anticipated for the 1288 keV excited state of ^{17}Ne .

IV. EXPERIMENTAL SETUP

The experiment was performed in the Flerov Laboratory of Nuclear Reactions at JINR. The ^{18}Ne beam with energy 35 MeV/nucleon was produced in fragmentation of a 53A MeV primary beam of ^{20}Ne bombarding a 55.5 mg/cm^2 ^9Be target. The secondary beam was selected using the ACCULINNA fragment separator [16].

The standard set of beam diagnostic detectors included two plastic scintillators (for time-of-flight — ToF and energy loss — ΔE measurements) and two position-sensitive multiwire

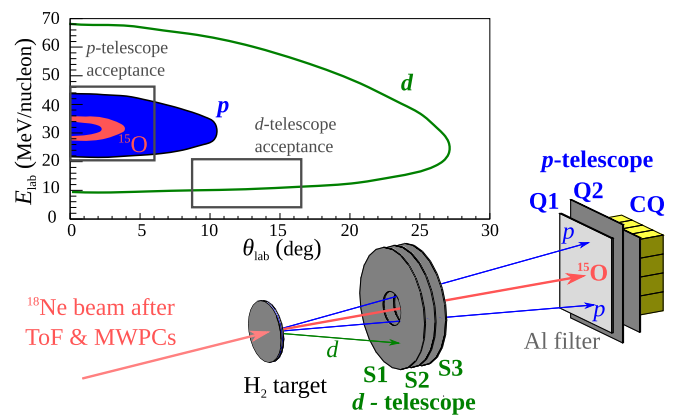


FIG. 3. The experimental setup and kinematic plot for the reaction products. Explanations are given in text.

chambers (for beam tracking). The data presented in this paper were collected in experiments carried out with a beam of total intensity on target of 2×10^5 pps. The part of ^{18}Ne ions in the beam cocktail was about 18%.

The secondary beam was focused on a cryogenic hydrogen target. The target was a cylindrical cell having the two $6\text{-}\mu\text{m}$ stainless-steel windows. Two versions of the target cell with different thicknesses were used in this experiment. The “thin” target, intended for work with hydrogen in the gaseous phase, had windows of 20 mm in diameter and a distance of 4 mm between them. The gas pressure in the target was 2 bar and the target was cooled to 24 K. The “thick” target, designed for operation with hydrogen in the liquid phase, had windows of 30-mm diameter and the effective thickness of 1.1 mm.

Figure 3 shows a schematic drawing of the detector setup. The annular telescope, located at 15-cm downstream the target (“thin” target case) and 12-cm downstream the target (“thick” target case), detected the recoil deuterons from the $^1\text{H}(^{18}\text{Ne},d)$ reaction. The telescope consisted of three position sensitive Si detectors with an inner (outer) radius of the sensitive area of 16 (41) mm and a thickness of 1 mm each. The first double-side silicon detector (S1) was segmented into 16 concentric rings on one side and 16 sectors on the other side. The two subsequent silicon strip detectors (S2 and S3), segmented into 16 sectors each, provided the measurement of total energy. Particle identification was performed by standard $\Delta E - E$ analysis. Each of the detector segments had its independent spectrometric channel. Signals from any sector of the S1 detector triggered the data acquisition system. An additional trigger (signal from the second ToF scintillator selected with a counting rate reduction of 4096) was used for beam monitoring.

Another telescope located on the beam axis at a distance of 30 cm from the target was intended for the detection of protons from the $^{17}\text{Ne}^* \rightarrow ^{15}\text{O} + 2p$ decay. The telescope consisted of two square $6 \times 6 \text{ cm}^2$, 1-mm thick silicon detectors (Q1 and Q2) segmented into 32 strips on one side. Following the pair of Si detectors installed was a wall of 16 CsI(Tl) crystals with PMT (Hamamatsu R9880U-20) readout (CQ). Each crystal was $1.6 \times 1.6 \text{ cm}^2$ across and had a thickness of 3.0 cm. To ensure the normal working conditions for the detectors a

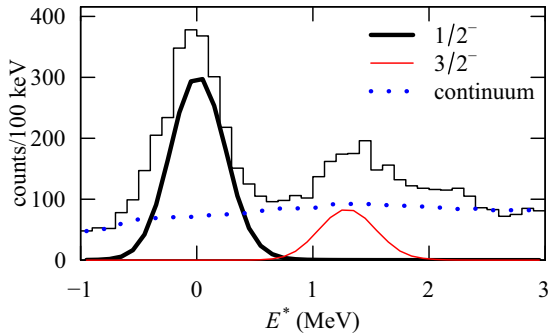


FIG. 4. Missing mass spectrum (histogram) of $^{17}\text{Ne}^*$ measured using the thin gas target in the angular range 4° – 18° in c.m.s. Lines show the calculated yields of the $1/2^-$ and $3/2^-$ states of ^{17}Ne and the estimated continuum background.

1.4-mm thick aluminum filter was installed directly in front of the telescope. This was enough to stop all the nuclei making the beam cocktail while the protons from the decay of $^{17}\text{Ne}^*$ lost only a small part of their energy in the aluminum filter.

V. DATA ANALYSIS

The first part of this experiment was made with thin (gaseous) target. A total flux of 7.4×10^9 bombarding ^{18}Ne nuclei passed through the hydrogen target with thickness $4.8 \times 10^{20} \text{ cm}^{-2}$. Figure 4 shows the missing mass spectrum of ^{17}Ne obtained as a result of this study of $^1\text{H}(^{18}\text{Ne}, d)^{17}\text{Ne}$ reaction. One can see in this spectrum the separate peak corresponding to the ^{17}Ne ground state and the bump with its left side centered close to the position of the first ($J^\pi = 3/2^-$) excited state. These structures are superimposed on the smooth continuum appearing mainly due to the reactions on the target windows. The bump is centered close to the position of the first excited state ($J^\pi = 3/2^-$), which points on the low population of the nearest $5/2^-$ and $1/2^+$ states. Therefore one can sort out only the peak corresponding to the contribution of $3/2^-$ state to the measured spectrum.

The measured missing mass spectrum allows us to make a good estimation of the ground-state yield, $N = 1635(52)$. Around one-third of that value makes the number of events responsible for the peak attributed to the $3/2^-$ state population. To reliably estimate the yield ratio of the two states [the $J^\pi = 1/2^-$ ground state (g.s.) and the $J^\pi = 3/2^-$ first excited state] we carried out the two-step DWBA calculations of $^{18}\text{O}(d, ^3\text{He})$ and $^{18}\text{Ne}(p, d)$ proton (neutron) pick-up reactions. The existing experimental data on the angular dependence of the $^{18}\text{O}(d, ^3\text{He})$ reaction differential cross sections at 52 MeV [17] were reanalyzed and, using a common exit ^3He optical model (OM) potential for these states, the ratio of spectroscopic factors (SFs) of the first excited state of ^{17}N to that of the ground state was obtained. In the case of the $^1\text{H}(^{18}\text{Ne}, d)^{17}\text{Ne}$ reaction studied in the present work we consider only the reaction channels populating the $1/2^-$ g.s. and the $3/2^-$ excited state. In a way similar to the isobaric-analogue case, the cross sections for the $^{18}\text{Ne}(p, d)$ reaction were calculated. The OM parameters for the reaction entrance channel were taken from the CH89 global nucleon-nucleus

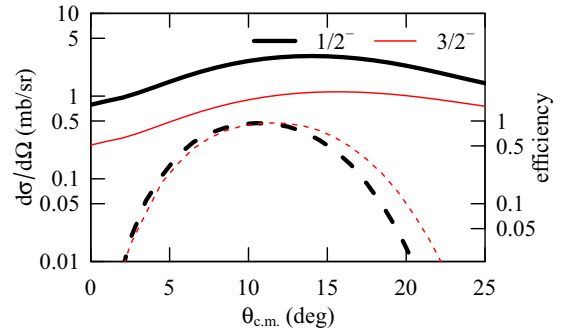


FIG. 5. Calculated differential cross sections in c.m.s. for the ^{17}Ne states obtained in the $^1\text{H}(^{18}\text{Ne}, d)^{17}\text{Ne}$ reaction (solid lines) and the corresponding detection efficiencies provided for deuterons emitted in the individual reaction channels (dashed lines).

potential algorithm. For the exit channels the CH89 potentials for the proton and neutron were folded to obtain the deuteron OM potential for the energy corresponding to the ^{17}Ne g.s. The same potential was applied to the ^{17}Ne first excited state. The resulting differential cross section values were multiplied by the corresponding factors emerging from the analysis of data known for the $^{18}\text{O}(d, ^3\text{He})$ reaction.

Figure 5 shows the calculated differential cross sections in the center-of-mass system for the $1/2^-$ and $3/2^-$ states of ^{17}Ne . The detection efficiencies for the population of these states were obtained by the Monte Carlo simulation. The corresponding curves are shown in Fig. 5 by dashed lines.

The yield obtained in our experiment for the ^{17}Ne ground state agrees within $\pm 10\%$ with that coming out from the differential cross section calculated with a value of 1.2 assumed for the spectroscopic amplitude (lines in Fig. 4 show the calculated yields of these states, and the calculated differential cross sections are shown in Fig. 5). The significant result for our further analysis is the conclusion that one can rely on the cross section values given in Fig. 5 for the reaction $^1\text{H}(^{18}\text{Ne}, d)^{17}\text{Ne}(J^\pi = 3/2^-)$.

When analyzing the data collected in the thick-target experiment we took into account the d - p - p coincidence events detected under the condition that the ^{18}Ne beam nuclei hit the central part of the hydrogen target within a circle with diameter of 18 mm. This choice eliminated the background caused by protons scattered from the material at the edges of the target windows. The so-selected beam flux made 2×10^{10} ^{18}Ne nuclei passing through the hydrogen target with thickness $4.6(4) \times 10^{21} \text{ cm}^{-2}$. In total, 660 d - p - p coincidence events were detected in this experiment.

Analysis took into account the energy and the trajectories (angles) of ^{18}Ne projectiles on the target. These parameters were measured with accuracy 1.5% and 2 mrad, respectively. It was supposed that the origin of all observed events was in the middle plain of the target. The triple coincidence events were detected in the center-of-mass angular range 3° – 24° , and their detection probability in small angular bins was estimated numerically. The values of the missing mass and combined mass energies, E_{miss}^* and E_{comb}^* , emerging from the data of each event were found.

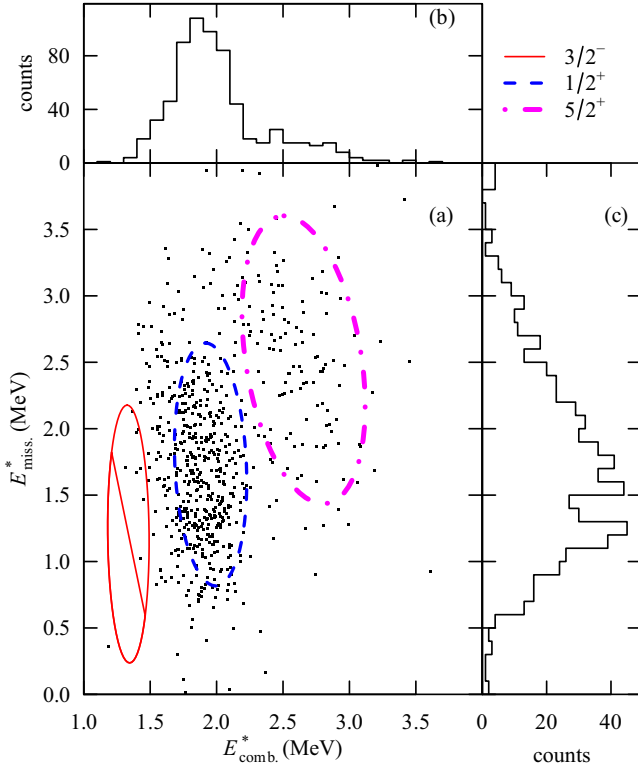


FIG. 6. Excitation energy spectrum of ^{17}Ne . (a) Correlation plot showing the excitation energy of ^{17}Ne measured by the missing mass method (E_{miss}^*) versus the energy obtained by the combined mass method (E_{comb}^*). The ellipses shown by solid red, dashed blue, and dash-dotted magenta curves correspond to the loci where the observation of 68% of events for the $3/2^-$, $1/2^+$, and $5/2^+$ states, respectively, is expected. (b) Combined mass spectrum, (c) missing mass spectrum.

The obtained spectra are presented in Fig. 6. In Fig. 6(a) the 660 events are displayed in their positions in the E_{miss}^* versus E_{comb}^* plot. Projections of this two-dimensional plot on its axes are the combined mass and missing mass spectra which are presented in Figs. 6(b) and 6(c). Poor resolution obtained in the missing mass spectrum emerges from the distortion caused by the thick target.

The combined mass for each individual d - p - p coincidence event is defined as the ^{17}Ne decay energy obtained as the sum of the center-of-mass energies of the two emitted protons. The small correction for the ^{15}O recoil energy is taken into account. In addition to the energies and emission angles of the two protons measured well in laboratory system the analysis requires a good knowledge of the momentum vector of ^{17}Ne produced in the $^1\text{H}(^{18}\text{Ne},d)^{17}\text{Ne}$ reaction. Of key importance here is the emission direction (polar angle) of the recoil deuteron measured in the experiment with 8 mrad precision. This defines the energy and polar angle of ^{17}Ne with accuracy 0.03% and 2 mrad, respectively.

The following procedures were implemented in the data analysis. The excitation energy of ^{17}Ne is separated in two parts: the energy of relative motion of two protons (E_x) and the relative-motion energy of the core and diproton (E_y). The

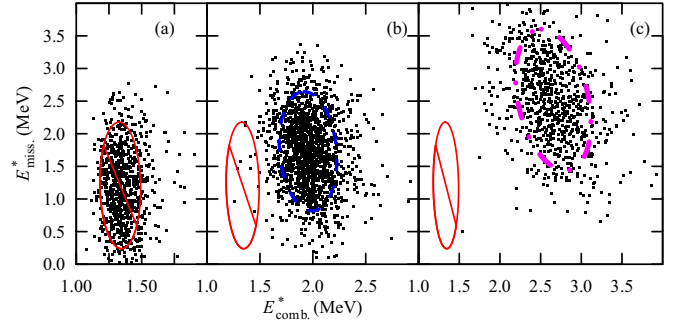


FIG. 7. Two-dimensional plots E_{miss}^* vs E_{comb}^* obtained as a result of Monte Carlo simulations. Shown in panels (a), (b), and (c), respectively, are simulations made for events coming individually from the $2p$ decay of the three ^{17}Ne states: $3/2^-$ (800 events), $1/2^+$ (1600 events), and $5/2^+$ (880 events). The loci outlined in Fig. 6(a) are also shown here.

value E_x for each individual event is defined from the proton momentum vectors measured in the laboratory system. Switching to the ^{17}Ne center-of-mass frame the ^{15}O momentum is also found according to momentum conservation, and E_y emerges from the defined ^{15}O momentum. The accuracy of the derived E_x and E_y values is limited by errors occurring at the transition from the laboratory system to the center-of-mass system.

The combined mass energy $E_{\text{comb}} = E_x + E_y$ has accuracy better than the missing mass. This makes perceptible the two states of ^{17}Ne (the states with $J^\pi = 1/2^+$, $E^* = 1916$ keV, and $J^\pi = 5/2^+$, $E^* = 2651$ keV) situated above its $2p$ -decay threshold [see Figs. 6(a) and 6(b)]. We cannot exclude that a few tens of events connected with the ^{17}Ne $5/2^-$ state are present in the spectrum in Fig. 6, but these are indistinguishable among the overwhelming number of the $1/2^+$ events and do not affect the further analysis. The event localization obtained in this experiment in the two-dimensional plot E_{miss} versus E_{comb} was tested by Monte Carlo (MC) simulations incorporating the standard GEANT4 [18,19] electromagnetic physics set for the description of particle interaction with matter. The simulation resulted in the definition of the loci where the majority of events (68%) associated with the ^{17}Ne excited states are localized (see Fig. 7). One can see in Fig. 6(a) that the event pattern obtained in experiment is described rather well by the simulation. Moreover the event distribution outside the loci obtained in the simulation is close to the experimental distribution. The superimposition of Figs. 7(b) and 7(c) describes the event seeding towards the low-energy tail of the combined mass spectrum, which is seen clearly in Fig. 6(a). The main origin of these seeding events was the small fraction of protons scattered from the passive area of annular telescope intended for the deuteron detection (see this in Fig. 3).

VI. WIDTH RATIO EVALUATION

The $\Gamma_{2p}/\Gamma_\gamma$ value can be evaluated by the following equation:

$$\frac{\Gamma_{2p}}{\Gamma_\gamma} = \frac{N_{2p}}{\varepsilon_{2p}N}, \quad (2)$$

where N_{2p} is the number of measured d - p - p events; N is the total number of events where ^{17}Ne was produced in its first excited $3/2^-$ state; ε_{2p} is the detection efficiency of the two protons emitted by ^{17}Ne . The value of ε_{2p} was estimated by means of the Monte Carlo simulation. The N value was estimated from the cross section shown in Fig. 5

$$N = N_B N_{\text{at}} \int \varepsilon \frac{d\sigma}{d\Omega} d\Omega = 38(6) \times 10^3,$$

where N_B is the number of ^{18}Ne beam nuclei hitting the target in this experiment; N_{at} is the effective thickness of liquid hydrogen target; ε is the efficiency of deuteron detection obtained from the Monte Carlo simulation of the setup.

The main problem of N_{2p} estimation is that there is no peak associated with the $3/2^-$ state in the $2p$ -coincidence spectrum, see Fig. 6(b). The spectrum shows some events near the energy of the $3/2^-$ state. Events located in the $3/2^-$ state energy range can be connected with this state as well as with the decay of the higher-lying excited states, and there is no way to clearly separate them. Therefore we can only set an upper limit for the $\Gamma_{2p}/\Gamma_\gamma$ ratio of the $3/2^-$ state.

The excitation energies obtained in the combined mass method ($E_{\text{comb.}}^*$) and missing mass method ($E_{\text{miss.}}^*$) should show some correlation. In particular, events occurring at excitation energy $E_{\text{miss.}}^* > 2.2$ MeV in the spectrum of Fig. 6(c) have nothing to do with the $3/2^-$ state population. Therefore it is appropriate to inspect the locus of this state in the two-dimensional plot in Fig. 6(a) shown in coordinates $E_{\text{comb.}}^*$ versus $E_{\text{miss.}}^*$. The solid ellipse shows the locus, where 68% of $3/2^-$ state decay events are concentrated. One can see eight events in this locus, which corresponds to $\Gamma_{2p}/\Gamma_\gamma < 6(1) \times 10^{-4}$. However, the majority of these events are located in the top-right part of the ellipse. The simulation presented in Fig. 7(a) shows that the line $E_{\text{miss.}}^* = 7.7 - 4.9E_{\text{comb.}}^*$ divides the $3/2^-$ locus by two equal parts containing 47 (bottom) and 53 (top) percent of events in the ellipse. If we reduce the $3/2^-$ locus in Fig. 6(a) to the bottom-left half of the ellipse we obtain no events in this region at all. This gives a lower limit $\Gamma_{2p}/\Gamma_\gamma < 1.6(3) \times 10^{-4}$.

VII. PROSPECTS TO IMPROVE SENSITIVITY LIMIT OF THE METHOD

As we can see the $2p$ -decay width limit achieved for the first excited state of ^{17}Ne is still much higher than the up-to-date theoretical predictions [11,14] give. It is natural to address a question: which $2p$ -width limit is attainable just by a realistic optimization of the setup. We assume here that a ^{18}Ne beam intensity of 10^6 s $^{-1}$ hitting the hydrogen target will be available, and one should optimize only the energy resolution to get rid of the background coming from the higher-lying excited states.

Figure 8 shows the Monte Carlo simulations of the “improved” setup. The prime parameters of the setup which affect the energy resolution are target thickness, energy, and angular resolutions of the charged particle telescopes. The optimized setup has gaseous hydrogen target with thickness of 1.2 mg/cm 2 . A supposition was made that the used recoil-deuteron detector array ensured measurements for the

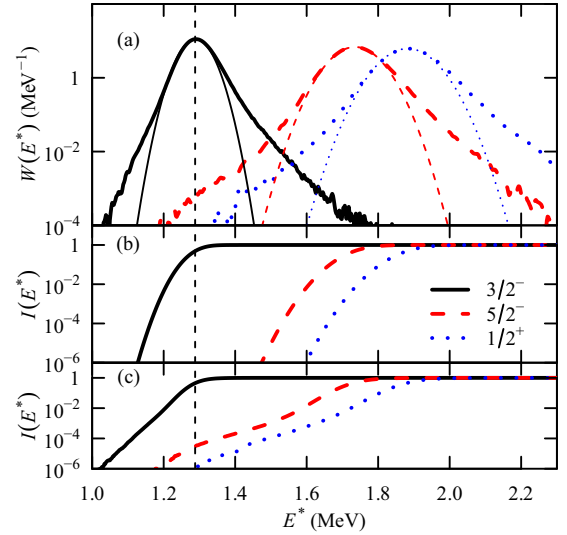


FIG. 8. Monte Carlo simulations of the improved setup demonstrating potential sensitivity limit of the method. The $3/2^-$, $5/2^-$, and $1/2^+$ contributions are shown by solid black, dashed red, and dotted blue curves, respectively. Panel (a) shows the probability density W . Thin curves give the Gaussian fits with respective deduced FWHM values of 80, 130, and 140 keV. Panels (b) and (c) show the cumulative distribution functions I for the Gaussian fits and for the complete MC distributions, respectively.

$^1\text{H}(^{18}\text{Ne},d)^{17}\text{Ne}$ reaction taking place in an angular range of $8^\circ \leq \theta_{\text{c.m.}} \leq 24^\circ$.

Standard GEANT4 electromagnetic physics set was used for particle interaction with matter description. Figure 8(a) shows the Monte Carlo simulation results normalized to the unity probability density $W(E^*)$ for the $3/2^-$, $5/2^-$, and $1/2^+$ states. The respective energy resolutions are 80, 130, and 140 keV (FWHM). Figures 8(b) and 8(c) show the cumulative distribution functions

$$I(E^*) = \int_{-\infty}^{E^*} W(E) dE,$$

for Gaussian fits of Fig. 8(a) and for full MC results, respectively.

If we look at the FWHM values only, the achieved resolutions are more than sufficient for our task: the states are very far from overlap, which is confirmed by Fig. 8(b). However, it can be seen in Fig. 8(a) that the behavior of the distribution “wings” deviates from the Gaussian profile at certain level and extends much further, beyond the actual resonance position than expected from the resonance FWHM. It can be found in Fig. 8(c) that the cumulative contribution of the “background” events from the $5/2^-$ and $1/2^+$ states is substantial in the energy region of the $3/2^-$ resonance, achieving $10^{-4} - 10^{-5}$. Figure 8(c) gives a guideline how to optimize the “signal to noise” ratio for the measurements aiming at the $3/2^-$ state decay: we should make a cutoff for $3/2^-$ events below a certain energy E^* . If we recall that the population of the $5/2^-$ state is at least one order of magnitude smaller than that for the $3/2^-$ state in the (p,d) reaction, an optimistic background condition 4×10^{-6} is obtained. This is quite close to the theoretical

limit $\Gamma_{2p}/\Gamma_\gamma \sim (0.9 - 2.5) \times 10^{-6}$ showing that direct $2p$ measurements could be feasible, at least from the background point of view.

It is clear that precise behavior of the “non-Gaussian” component of the energy resolution is a very delicate issue depending on the fine details of the experimental apparatus. Here we demonstrate that (i) this issue can be overcome in a realistic scenario and the further search for the $2p$ branch in ^{17}Ne $3/2^-$ state is feasible and (ii) the prior careful studies of this aspect of the planned experiment are unavoidable.

We should also point out that additional background-elimination method can further improve the situation here. This is connected with the energy correlation analysis as provided by Fig. 6(a). A six-fold improvement was achieved for the $\Gamma_{2p}/\Gamma_\gamma$ limit in the current experiment, and it can be evaluated that even higher improvement factors are possible depending on the details of the experimental setup.

From a more general point of view, in the particular case of our experiment we aimed to determine the $\Gamma_{\text{part}}/\Gamma_{\text{tot}}$ ratio for the quite complicated $2p$ decay process. It is clear that in the easier cases of states decaying via proton or alpha emission the $\Gamma_{\text{part}}/\Gamma_{\text{tot}}$ ratio attainable in this approach should be much better.

VIII. CONCLUSION

We performed a dedicated search for the $2p$ decay branch of the first excited $3/2^-$ state of ^{17}Ne populated in the $^1\text{H}(^{18}\text{Ne},d)^{17}\text{Ne}$ transfer reaction. The population of low-energy states ($E^* < 3$ MeV) in the ^{17}Ne nucleus was also studied. Based on these results the new upper limit $\Gamma_{2p}/\Gamma_\gamma \leq 1.6(3) \times 10^{-4}$ is established. This significantly (about a factor of 50) reduces the value of the limit defined in the previous work [15]. The strong improvement of the $\Gamma_{2p}/\Gamma_\gamma$ limit was achieved due to the choice of the transfer reaction used as a

tool for the two-proton decay study of $^{17}\text{Ne}^*$ and application of the original “combined mass” method to the reconstruction of the ^{17}Ne excitation spectrum. The latter allowed us to improve significantly the instrumental resolution in the measurements made with the thick target. The measured limit for the rate value rules out the predictions made for the $2p$ decay width of the ^{17}Ne first excited state by the simplified diproton decay model [13], but it is still insufficient to be restrictive for the realistic theoretical predictions [11,14].

We see prospects for a considerable (by one to two orders of magnitude) reduction of the $\Gamma_{2p}/\Gamma_\gamma$ upper limit in the proposed experimental method without revolutionary modification of the setup. Such improvements open a way to the direct experimental observation of the true, radioactive $2p$ -decay of the ^{17}Ne $3/2^-$ state taking the theoretically predicted ratio of $\Gamma_{2p}/\Gamma_\gamma \sim (0.9 - 2.5) \times 10^{-6}$ as a trusted aim.

The issue of general interest is the development of methods applicable to the studies of weak particle (alpha, proton, or two-proton) decay branches of excited states that reside well below the Coulomb barrier and thus have extremely small $\Gamma_{\text{part}}/\Gamma_\gamma$ ratios. The possibility to derive directly such weak decay branches in one experiment makes promising the application of the proposed approach to the problems of nuclear astrophysics.

ACKNOWLEDGMENTS

A.A.B., S.A.R., T.A.G., A.V.G., I.A.E., S.A.K., A.G.K., and P.G.S. are supported by the Helmholtz Association under Grant Agreement IK-RU-002. This experiment was partly supported by the RSF 17-12-01367 Grant and MEYS Projects (Czech Republic) LTT17003 and LM2015049. The authors are grateful to Profs. Yu. Ts. Oganessian and S. N. Dmitriev for support to this work; helpful discussions with Dr. I. Mukha are acknowledged as well.

-
- [1] W. A. Fowler, G. R. Caughlan, and B. A. Zimmerman, *Ann. Rev. Astr. Astrophys.* **5**, 525 (1967).
 - [2] V. Guimarães, S. Kubono, M. Hosaka, N. Ikeda, S. C. Jeong, I. Katayama, T. Miyachi, T. Nomura, M. H. Tanaka, Y. Fuchi, H. Kawashima, S. Ohkawa, S. Kato, H. Toyokawa, C. C. Yun, T. Niizeki, K. Ito, T. Kishida, T. Kubo, Y. Pu, M. Ohura, H. Orihara, T. Terakawa, S. Hamada, M. Hirai, and H. Miyatake, *Nucl. Phys. A* **588**, c161 (1995).
 - [3] V. Guimarães, S. Kubono, M. Hosaka, N. Ikeda, M. H. Tanaka, T. Nomura, I. Katayama, Y. Fuchi, H. Kawashima, S. Kato, H. Toyokawa, T. Niizeki, C. C. Yun, T. Kubo, and M. Ohura, *Z. Phys. A* **353**, 117 (1995).
 - [4] M. V. Zhukov, I. J. Thompson, and the Russian-Nordic-British Theory (RNBT) Collaboration, *Phys. Rev. C* **52**, 3505 (1995).
 - [5] L. V. Grigorenko, I. G. Mukha, and M. V. Zhukov, *Nucl. Phys. A* **713**, 372 (2003).
 - [6] L. V. Grigorenko, Y. L. Parfenova, and M. V. Zhukov, *Phys. Rev. C* **71**, 051604 (2005).
 - [7] J. Marganec, T. Aumann, M. Heil, R. Plag, and F. Warners (for the LAND-R³B Collaboration), *J. Phys.: Conf. Ser.* **337**, 012011 (2012).
 - [8] J. Marganec *et al.*, *Phys. Lett. B* **759**, 200 (2016).
 - [9] J. Görres, M. Wiescher, and F.-K. Thielemann, *Phys. Rev. C* **51**, 392 (1995).
 - [10] L. V. Grigorenko and M. V. Zhukov, *Phys. Rev. C* **72**, 015803 (2005).
 - [11] L. V. Grigorenko and M. V. Zhukov, *Phys. Rev. C* **76**, 014008 (2007).
 - [12] M. Pfützner, M. Karny, L. V. Grigorenko, and K. Riisager, *Rev. Mod. Phys.* **84**, 567 (2012).
 - [13] M. J. Chromik, B. A. Brown, M. Fauerbach, T. Glasmacher, R. Ibbotson, H. Scheit, M. Thoennessen, and P. G. Thirolf, *Phys. Rev. C* **55**, 1676 (1997).
 - [14] E. Garrido, A. S. Jensen, and D. V. Fedorov, *Phys. Rev. C* **78**, 034004 (2008).
 - [15] M. J. Chromik, P. G. Thirolf, M. Thoennessen, B. A. Brown, T. Davinson, D. Gassmann, P. Heckman, J. Prisciandaro, P. Reiter, E. Tryggstad, and P. J. Woods, *Phys. Rev. C* **66**, 024313 (2002).

- [16] A. Rodin, S. Sidorchuk, S. Stepantsov, G. Ter-Akopian, A. Fomichev, R. Wolski, V. Galinskiy, G. Ivanov, I. Ivanova, V. Gorshkov, A. Lavrentyev, and Y. Oganessian, *Nucl. Instrum. Methods B* **126**, 236 (1997).
- [17] D. Hartwig, G. T. Kaschl, G. Mairle, and G. J. Wagner, *Z. Phys.* **246**, 418 (1971).
- [18] S. Agostinelli *et al.*, *Nucl. Instrum. Methods A* **506**, 250 (2003).
- [19] J. Allison *et al.*, *IEEE Trans. Nucl. Sci.* **53**, 270 (2006).